THE AMERICAN SOCIETY OF MECHANICAL ENGINEERS
Three Park Avenue, New York, N.Y. 10016-5990

99-GT-408

COMPARISON OF THEORETICAL AND EXPERIMENTAL DATA FOR AN OSCILLATING TRANSONIC COMPRESSOR CASCADE

Volker Carstens
Institute of Aeroelasticity
DLR
Göttingen, Germany

Stefan Schmitt
Institute of Propulsion Technology
DLR
Köln, Germany

ABSTRACT

Numerical and experimental results are compared for a compressor cascade performing harmonic oscillations in transonic flow. The flow field was calculated by a Q3D Navier Stokes code, the basic features of which are the use of an upwind flux difference scheme for the convective terms, the implementation of an effective one-equation turbulence model and the use of deforming multi-block grids. The experimental investigations were performed in an annular cascade windtunnel where unsteady blade pressures were measured for two different operating conditions of the cascade.

The present data were all obtained for tuned torsional modes where the blades performed pitching oscillations with the same frequency and amplitude, but with a constant interblade phase angle. In the first test case the steady flow around the blades was purely subsonic. For the second test case the compressor cascade was run under transonic flow conditions where a normal shock in the front part of the blades' suction side is followed by a blade passage shock.

It becomes apparent that under subsonic flow conditions the predicted aerodynamic damping coefficients are in resonable agreement with the experimental data, although the numerical pressure amplitudes are much higher than the measured ones. In transonic flow significant discrepancies between computed and experimentally determined pressure amplitudes are observed, whereas the accuracy of the pressure phase prediction is comparable to the subsonic test case. Another important result of these investigations is that oscillations of the blade passage shock lead to strong variations of the local aerodynamic damping of the blades, but do not significantly change the global damping coefficient of the tested compressor cascade.

INTRODUCTION

The development of modern aircraft engine compressors with increased pressure ratio and reduced weight led to highly loaded stages with transonic inflow. As a result, the design engineers of a completed engine often encountered severe aeroelastic problems, the solution of which could be difficult and costly. Therefore, tools are needed which are able to correctly predict the aeroelastic behaviour of the blading already in the design process.

The quality of the aeroelastic analyses of turbomachine blades strongly depends on the underlying aerodynamic model of the flow. The accurate and efficient calculation of the unsteady airloads acting on vibrating blades is a fundamental prere-quisite to predict the flutter and forced vibrations of a given blade assembly. For this reason, much theoretical work has been done in the last decade to develop methods which are able to reliably compute the pressure distribution around oscillating blades for the determination of the aerodynamic damping.

The unsteady aerodynamic codes developed up to the present can be roughly divided into two groups, namely linear and nonlinear methods. Linearized methods assume the unsteadiness in the flow to be a small disturbance of a mean steady flow and they approximate the full Euler or Navier-Stokes equations by a set of linear equations for the unsteady flow values. These simplified analyses meet the requirement of computational efficiency and have been widely used for standard routine aeroelastic design studies.

Linearized Euler methods have been presented by Hall and Crawley (1989), Kahl and Klose (1993), Hall and Lorence (1993) and Montgomery and Verdon (1997). Further progress

Presented at the International Gas Turbine & Aeroengine Congress & Exhibition
Indianapolis, Indiana — June 7–June 10, 1999

has been gained by taking into account viscous effects. The papers of Clark and Hall (1995) and Holmes et. al. (1997) are examples for the application of a linearized analysis to viscous flows. However, the basic drawback of such methods is their lacking ability to treat important physical features such as large amplitude vibration, strong moving shocks and flow separation.

The steadily growing power of computers has stimulated the development of numerical methods for solving full nonlinear equations. Although these methods are far from being a standard tool for routine investigations, they help to understand and assess the nonlinear phenomena occuring in an unsteady flow caused by blade vibrations. Such nonlinear approaches have been presented for inviscid flows, e.g., by Gerolymos (1988,1993), He (1989), Carstens (1993), Peitsch et al. (1994) and Chuang and Verdon (1998), whereas He (1993), Abhari and Giles (1995), Ayer and Verdon (1996), Grüber and Carstens (1996) and Weber et al. (1997) have published contributions to the solution of the unsteady Reynolds-averaged Navier-Stokes equations.

Usually the quality of theoretical results is judged by comparing them with experimental data. For this purpose Bölcs and Fransson published in 1986 the experimental results of a set of cascade standard configurations which were extensively investigated in the years that followed. The remarkable conclusion which may be drawn from these investigations is that most of the existing numerical methods are able to correctly predict the aeodynamic damping of vibrating blades for subsonic flow in the absence of strong viscous effects, but often fail to predict reasonable results for flows which are characterized by the occurence of shocks or flow separation.

The aim of this paper is to study a typical nonlinear effect in cascade flows, namely the influence of a shock on the aerodynamic damping of a transonic compressor cascade. This phenomenon has been investigated by Hennings and Belz (1998) in a basic experiment which indicates that a strong oscillating shock may significantly change the aerodynamic damping of a blade. The experimental investigations were performed at the Laboratoire de Thermique Appliquée et de Turbomachines (LTT) of the EPF-Lausanne. Unsteady blade pressures were measured in an oscillating compressor cascade at subsonic and transonic flow conditions. The corresponding theoretical results were computed by the TRACE code developed by Eulitz, Engel et. al. (1993,1996,1998). Experimental and theoretical results of unsteady pressures and damping coefficients are compared for the two already mentioned flow conditions and are investigated with respect to the aerodynamic stability of the cascade.

NUMERICAL METHOD

The set of flow equations used here are the quasi-three-dimensional unsteady compressible Reynolds-averaged Navier-Stokes equations in transformed coordinates. The strong conservation law form of these equations can be written as:

$$h\,\partial_\tau \hat{Q} + \partial_\xi h\,(\hat{F} - \hat{F}_v) + \partial_\eta h\,(\hat{G} - \hat{G}_v) = \hat{S} \qquad (1)$$

The details of the state vector $\hat{Q}$, the inviscid fluxes $\hat{F}$ and $\hat{G}$ and the viscous fluxes $\hat{F}_v$ and $\hat{G}_v$ are explained in Eulitz et.al. (1996). The source term $\hat{S}$ on the right hand side of (1) accounts for varying streamtube thickness on a constant radius in a non-rotating frame of reference.

The time integration of equations (1) for the flow around vibrating blades is performed according to the two-grid acceleration technique proposed by He (1993). This time-stepping technique is combined with a second-order-accurate four-stage Runge Kutta scheme.

The spatial discretization of the inviscid fluxes $\hat{F}$ and $\hat{G}$ is ohtained by using Roe's upwind scheme (1989) in combination with van Leer's MUSCL extrapolation. Here the primitive variables density, flow velocity and pressure are extrapolated according to a second order scheme. The spatial derivatives of the viscous fluxes $\hat{F}_v$ and $\hat{G}_v$ are approximated by central differences.

The Reynolds-averaged equations (1) are closed with the one-equation turbulence model by Spalart and Allmaras (1992). This model solves a transport equation for a quantity related to the eddy-viscosity μ_t. Numerous numerical studies have indicated that this turbulence model is numerically robust and independent of the grid. It produces results of reasonable accuracy for unsteady and mildly separated flows and is capable of yielding results which are superior to those of standard two-equation models. No transition model has been used in the present study, the start of turbulent flow is initiated at certain stations on the suction and pressure sides of the blades.

For turbomachinery flows, the system (1) of Navier-Stokes equations has to be supplied with boundary conditions at the blades surfaces, the in- and outflow boundaries and the periodic boundaries of the computational domain. On the blades surfaces the flow velocity is equated with the blade velocity (no slip condition). In order to completely determine the wall fluxes, two further equations are needed which prescibe the thermodynamic variables at the wall. First of all, the wall temperature is calculated by assuming adiabatic walls which require a vanishing normal temperature gradient at the wall. Secondly, the surface pressure is computed from the normal momentum equation which yields the normal pressure gradient as function of the blade acceleration and the derivatives of the velocity.

The implementation of the in- and outflow boundary conditions is accomplished by a method proposed hy Giles (1988). The hasic idea of this procedure is to develop the solution vector on the boundary into spatial Fourier series. A linearization of the eigenvectors of this Fourier decomposition yields a system of equations which can be directly implemented into the time-space integration of the interior field solution. For steady flow the zero mode is coupled to the prescribed boundary conditions and the higher harmonics are modelled in a non-reflecting sense, whereas the unsteady flow is exclusively computed with non-reflecting boundary conditions.

The application of periodic boundary conditions is self-evident with the used line-period multi-block grid in combination with a the multi-channel method (see next section).

GRID GENERATION FOR MOVING BLADES

The grid generation needed to compute the solution of the Navier-Stokes algorithm in a boundary-fitted coordinate system is obtained by an elliptic grid generation code based on the solution of Poisson equations, the basic feature of which is the possibility to control the line spacing and intersection angle of the grid lines at the physical boundaries. The code mentioned above allows for an arbitrary decomposition of the computational domain into blocks, a feature which avoids strong mesh distortions and which advantageously effects the capturing of flow phenomena such as shocks or wakes.

The type of grid used for the cascade flow calculation is a line-periodic multi-block grid, where each grid point on the lower channel boundary has its counterpart on the upper channel boundary in the pitchwise direction. Only the block surrounding the blade has been generated as an O-grid with a high density of grid lines at the blade surface, while all the other blocks consist of H-grids. Hence, any code is easily introduced on the grid and the periodic boundary conditions can be imposed in a natural way.

The grid point displacement must be carefully organized for oscillating blades. As the blades are in relative motion to each other, the total grid has to be deformed to enable it to conform to the new position of the vibrating blades after each time step. In order to make the used grid generation code capable of steadily deforming the single blocks of the whole mesh, the following procedure has been implemented into the code :
In a first step the block boundaries are deformed where the movement of the boundary representing the blade is prescribed. This is achieved by defining a maximum deformation radius inside of which all deformations are smoothly damped to zero, while the outer channel boundaries are kept fixed. A second step organizes the deformation of all grid lines within a given block by transfinite interpolation and - if necessary - additional elliptic iterations.

This method yields a reasonable control of the grid point speed in the interior field. For the given harmonic motions the time-dependent grid is computed by the harmonic interpolation (with respect to time) of a set of steady-state grids with different blade amplitudes.

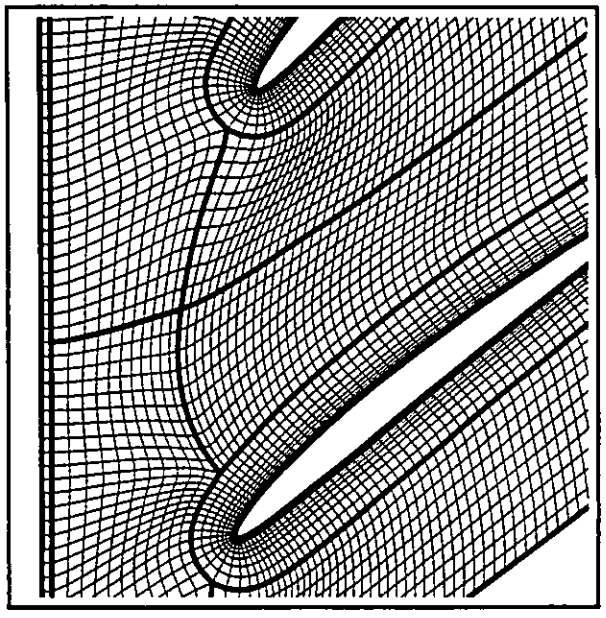

Figure 1: Close up of the deformed multi-block grid

Since with the present method the unsteady cascade flow is computed according to the so-called multi-channel method, the number of blade channels in which the flow has to be calculated depends on the oscillation mode of the cascade. Tuned modes with constant amplitude and constant interblade phase angle result in a pitchwise spatially periodic flow where the spatial periodic length is determined by the interblade phase angle σ. Consequently, an interblade phase angle of $\sigma = 180°$ requires two blade channels to compute the unsteady flow; four channels are sufficient for $\sigma = \pm 90°$, etc. **Figure 1** shows a deformed grid for tuned pitching oscillations with $\sigma = 180°$.

TEST FACILITY AND CASCADE GEOMETRY

The experimental tests on the compressor cascade presented below were performed in the non-rotating annular cascade windtunnel at the Laboratoire de Thermique Appliquée et de Turbomachines (LTT) of the EPF-Lausanne (Bölcs 1983). In this test facility (**Figure 2**) the inflow Mach number can be

varied from low subsonic (M = 0.3) to supersonic values (M = 1.4), while the inflow angle can be regulated over a range of 50 degrees. The flow conditions are measures with aerodynamic probes and pressure taps. For time-dependent measurements

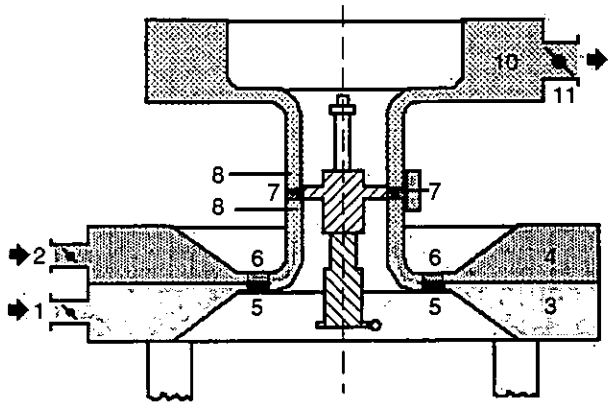

1,2 inlet valves
3,4 outer and inner setting chambers
5,6 outer and inner preswirl vanes
7 test cascade
8 aerodynamic probes
10 outlet chamber
11 outlet valve

Figure 2: Test facility for annular cascades

the blades in the test cascade are mounted on elastic springs and are driven into a vibration mode by means of a vibration control system (Schläfli 1989). Each blade mass is mounted on a spring-mass-system which has been designed and tuned to produce the same eigenfrequency for all 20 blades. The blades are forced into vibration by means of invidual magnetic exciters, each with its own feed-back loop.

Steady pressures are measured by nine pressure tabs on the suction side and nine on the pressure side of a blade. Unsteady pressures were recorded with an overall equipment of nineteen pressure transducers, ten of which are mounted on the suction side, the other nine on the pressure side. Installation on one blade is not possible for technical reasons, thus the transducers have been distributed over four blades. A special feature of the transducer installation is the concentration of eight transducers on the suction side (from the leading edge to fourty percent chord length) of one single blade. This rather dense distribution has been chosen to capture the dynamic pressure response of the blade to a moving shock.

The geometry of the used compressor test cascade consisting of twenty NACA 3506-profiles is depicted in **Figure 3.**

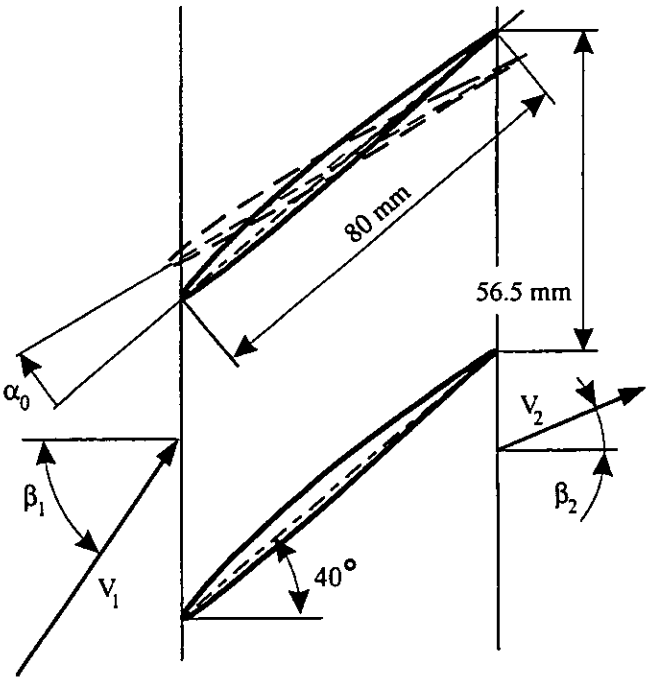

Figure 3: Geometry of compressor test cascade

PRESENTATION AND DISCUSSION OF RESULTS

Results for unsteady flow were computed for two different experimentally investigated test cases, namely a pure subsonic and a transonic flow configuration. The values of the steady mass averaged in- and outflow data are listed in Table 1.

	β_1	p_{t_1}	p_1	M_1	β_2	p_2
subs.	48.3°	1199 mb	824mb	0.75	40.9°	862 mb
trans.	49.6°	1343 mb	795mb	0.90	40.9°	809 mb

Table 1: Mass averaged in- and outflow data

Unsteady pressure distributions were measured for tuned pitching modes around mid-chord with a pitching amplitude of $\alpha_0 = 0.3°$, while the oscillation frequency of the blades was kept fixed at 225 Hz. The pressure signals were recorded and evaluated for all of the twenty possible interblade angles $\sigma = \frac{2\pi}{20}(j-1), j = 1, ..., 20$. Here the interblade phase angle is defined as such that it is positive if the phase of the adjacent blade on the suction side advances to the phase of the regarded blade. This means that a positive σ causes a traveling wave running from top to bottom, whereas a negative σ produces a wave in the opposite direction (see Fig. 3). Defining the reduced frequency by

$$\omega^* = \frac{2\pi f L}{V_1} \tag{2}$$

with f = frequency
L = blade chord length
V_1 = mass averaged inflow velocity,

we obtain $\omega^* = 0.4583$ for the subsonic and $\omega^* = 0.3915$ for the transonic flow case.

All theoretical results for steady and unsteady flow were computed with the multi-block H-grid of Figure 1 which consists of five blocks with an overall grid point number of 20299.

First of all, the computed results for steady flow must be checked, since they serve as initial solutions for the unsteady flow calculations. The steady pressure coefficient is defined with respect to the inlet values of total and static pressure as

$$c_p(s) = \frac{p(s) - p_1}{p_{t_1} - p_1} \tag{3}$$

with p(s) = variable static pressure on the blade
p_1 = static inlet pressure
p_{t_1} = total inlet pressure.

Before comparing experimental and theoretical steady pressure values, a few remarks should be made about the real flow in the annular cascade windtunnel. The real flow in the annular windtunnel distinctly shows three-dimensional characteristics such as a radial pressure gradient or a varying mass ratio per area from hub to tip, which are due to the increasing pitch-chord-ratio (from 0.63 to 0.79). Additionally, viscous effects such as wall boundary layers and corner stall cause three-dimensional flow patterns and may significantly influence the flow quantities at mid-span where the experimental data were recorded.

Assuming the unsteadiness in the flow as a disturbance of the steady mean flow, it is clear that no reliable results can be expected from a time-dependent computation if the predicted steady pressure distribution differs greatly from the measured one. The stream tube contraction used here approximately models the 3D-effects mentioned above; nevertheless, it should be emphasized that it is only a tool to fit the in- and outflow values of the computed solution to the measured ones and, in general, does not meet the real flow physics in the cascade.

Figure 4 shows the comparison between experimental and theoretical results for the subsonic test case. A stream tube contraction ratio of 1.20 was used to match the computed in- and outflow averaged pressure values to the data given in **Table 1**. The contraction was linear from the leading edge to the trailing edge. The agreement between theory and experiment is good on the pressure side of the blades, whereas some deviations between measured and predicted data are noticeable on the suction side. Here, the acceleration and deceleration of the real flow is not correctly reproduced by the computed results. Although the prediction method used is a viscous one the calculated outflow angle of 35.9° differs by 5° from the measured one (40.9°) and leads to a stronger curvature of the streamlines in the blade channel. This behaviour is similar to the investigations of Körbächer (1996). The experimental and theoretical results for the transonic test case are depicted in **Figure 5**. Here, the stream tube contraction

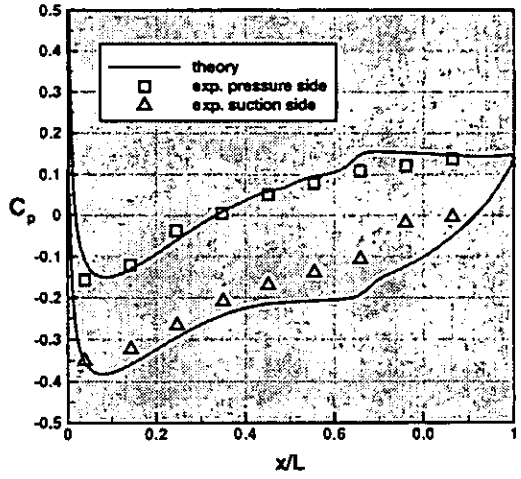

Figure 4: Steady pressure distribution, Ma1 = 0.75, $\beta_1 = 48.3°$

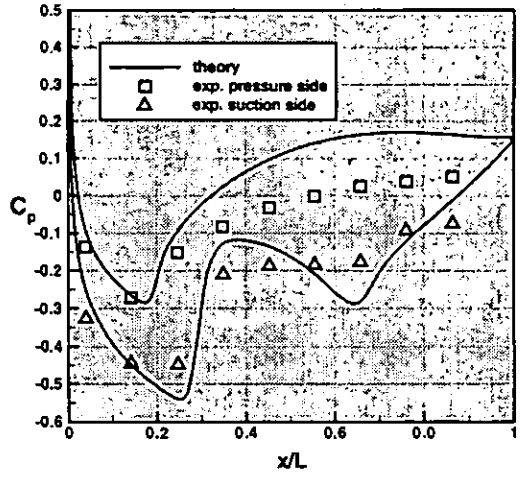

Figure 5: Steady pressure distribution, Ma1 = 0.90, $\beta_1 = 49.6°$

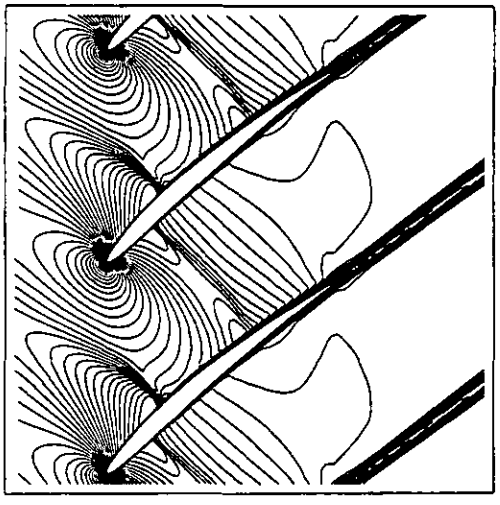

Figure 6: Iso-Machlines, Ma1 = 0.90

ratio was 1.21. The transonic flow through the blade channel is choked as seen by the iso-Machlines presented in **Figure 6**. After the occurence of a first shock on the suction side, the flow is accelerated again to produce a supersonic region in the blade channel which is terminated by a second shock. The locations where this shock impinges on the suction and pressure sides of the blade are clearly noticeable in the theoretical as well as in the experimental data.

In contrast to the previous case, the overall agreement between measured and predicted pressures is not satisfactory. Although both shocks on the suction side are captured well, the predicted strong acceleration to the second shock differs significantly from the moderately increasing measured pressure level. The predicted pressure coefficients on the pressure side are in agreement with the experimental values until the blade channel shock impinges onto this side of the blade, after which large deviations between theory and experiment are observed. This is obviously due to the fact that, as in the subsonic test case, the computed outflow angle differs by more than 4° from the measured one.

It must be stated that it is not possible to fit the experimental and numerical results very well over the whole blade. However, numerical tests showed that the agreement with a stream tube contraction was much better than with a pure 2D-computation.

The calculation of the unsteady flow quantities for tuned pitching modes was performed with the following technique : When at rest in the computed steady flow the blades start to move with the prescribed oscillation mode, while the number of blade channels to be computed is determined by the chosen interblade phase angle (IBPA). Calculating the unsteady clockwise defined moment coefficient per unit span from the unsteady pressure coeffient

$$c_p(s,t) = \frac{p(s,t) - p_1}{\alpha_0 \, (p_{t1} - p_1)} \,, \tag{4}$$

where α_0 denotes the pitching amplitude, by

$$c_M(t) = \frac{1}{L^2} \oint_0^{s_0} c_p(s,t) \, [(x(s) - x_0)\dot{x}(s) + (y(s) - y_0)\dot{y}(s)] ds \tag{5}$$

with x(s), y(s) = blade coordinates
$\dot{x}$(s), $\dot{y}$(s) = derivatives of blade coordinates
x_0, y_0 = coordinates of pitching axis,

the computation is stopped when periodic convergence of the aerodynamic work coefficient is achieved, i.e. when the integral

$$w(T) = \int_0^T c_M(t) \, \dot{\alpha}(t) \, dt = \oint_{\alpha(0)}^{\alpha(T)} c_M[\alpha(t)] \, d\alpha \,, \tag{6}$$

where T and $\alpha(t)$ denote the period and the time-dependent pitching angle, respectively, has converged to a steady value. Experience shows that this usually happens after 2-3 cycles of oscillation. Applying a Fourier analysis to the stored time-dependent pressure and moment coefficients for the last computed period, the first harmonics of these quantities were obtained and can be compared with the corresponding measured values. The unsteady pressure coefficient representing the first harmonic is then expressed as the complex number

$$c_{p_{H1}}(s) = \frac{\tilde{p}(s) \, e^{i\phi(s)}}{\alpha_0 \, (p_{t1} - p_1)} \tag{7}$$

with $\tilde{p}(s)$ = unsteady pressure amplitude
$\phi(s)$ = unsteady pressure phase.

Due to a limitation in the available computational resources, only three interblade phase angles were calculated for each of the test cases. These IBPA's were −90°, +90° and 180°. **Figures 7** and 8 show the comparison between computed and measured unsteady pressure distributions for the subsonic test case at the two interblade phase angles $\sigma = -90°$ and +90°. These values are depicted since the experiments indicated that they are close to the maximum and minimum damping IBPA's of the test cascade.

The results of the first harmonics are presented in a modulus-phase diagram. Both diagrams show a considerable overprediction of the pressure amplitudes, which can be attributed to the higher steady blade loading. Additionally, the relative maximum of the absolute pressure value at 60 percent of

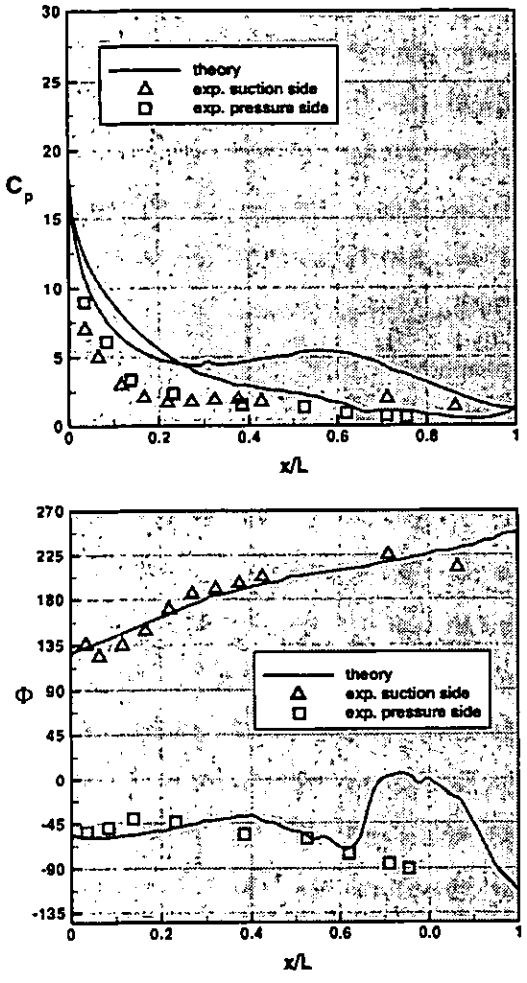

Figure 7: Unsteady pressure distribution, modulus and phase, Ma1 = 0.75, $\sigma = -90°$

blade chord is not found in the experimental data. A satisfactory agreement with the measured results is obtained for the phase lead or lag of the unsteady pressure with respect to the blade motion. Here, the predicted phase on the pressure and the suction side is close to the measured one for $\sigma = -90°$, whereas the computed results for $\sigma = +90°$ yield an overall smaller value on the suction side than that of the experimental data.

In order to judge the aerodynamic stability of the cascade the aerodynamic damping coefficient has been calculated. This coefficient is defined as the out-of-phase (imaginary) part of the moment coefficient and is easily computed by replacing $c_p(s,t)$ with $c_{p_{H1}}(s)$ in equation (20). **Figure 9** shows the measured and predicted aerodynamic damping as a function of the interblade phase angle. Although the computed maximum damping is twice as high as the measured one, the agreement of the experimental and theoretical value near the minimum damping is good.

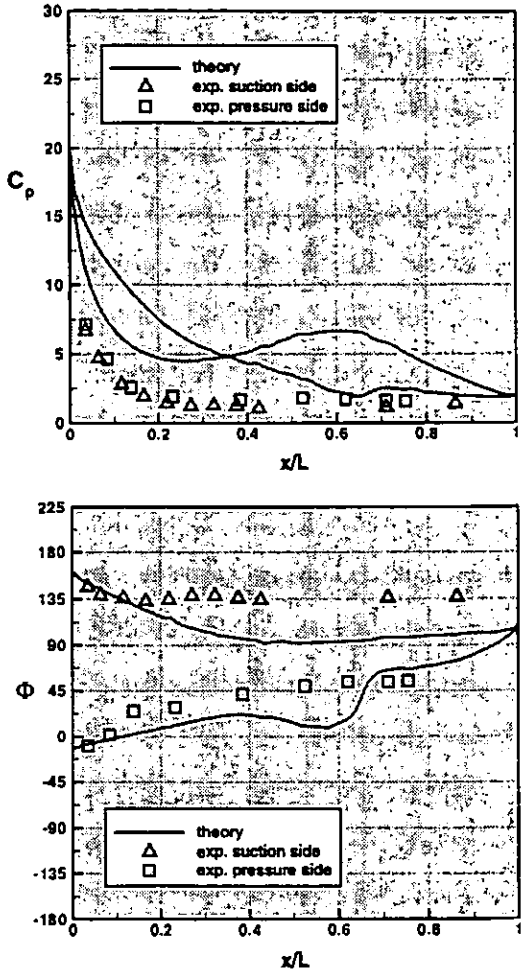

Figure 8: Unsteady pressure distribution, modulus and phase, Ma1 = 0.75, $\sigma = +90°$

The comparison between measured and predicted unsteady pressure data for the transonic test case is depicted in **Figures 10 and 11**. The computed pressure amplitudes yield a pronounced response to the front shock and the blade channel shock, where the width of the shock impulse is a measure for the amplitude of the shock oscillation on the suction and pressure sides, respectively. The response to the front shock produces a rather sharp peak, indicating a small shock amplitude, whereas the blade channel shock with the larger amplitude causes wider peaks. This is confirmed by **Figure 12** which shows the iso-Machlines in the blade channel at four subsequent time-steps for $\sigma = +90°$. The front shock appears at any time-step with only minimal changes in location and strength, whereas the blade channel shock is characterized by a rather large oscillation amplitude accompanied by drastic

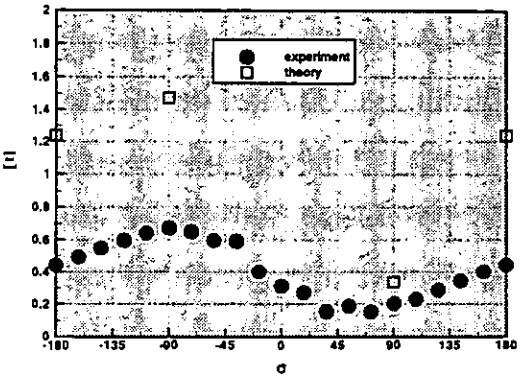

Figure 9: Aerodynamic damping coefficient versus interblade phase angle, subsonic flow

changes in its strength. After a quarter-period of the blade motion the shock has completely disappeared, after a further half-period it reaches his rearward position with maximum strength.

A similar behaviour is observed when computing the flow with the interblade phase angles $\sigma = -90°$ and $\sigma = 180°$, where the basic difference is the phase shift of the shock motion relative to the blade motion.

The scenario outlined above is only partly reflected by the experimental results. Due to the high density of pressure transducers in the front part of the suction side, the response to the front shock is clearly visible in the measured data. Unfortunately, the distribution of transducers was rather coarse at those locations where the blade channel shock impinges onto the suction and pressure sides. Consequently, no typical shock impulse is noticeable here.

Despite the strong discrepancies between the computed and measured pressure amplitudes, the agreement of predicted and experimentally determined pressure phases is satisfactory. A critical problem is obviously the correct prediction of the suction side pressure phase for $\sigma = +90°$. Here the agreement is quite good from the leading edge to a location just after the shock. Afterwards, the predicted phase lags significantly behind the measured one. It should be mentioned that the agreement of the pressure phases for $\sigma = 180°$ (not shown here) is similar to that of the depicted IBPA $\sigma = -90°$ (Fig. 10).

Finally, the aerodynamic damping coefficient for transonic flow is presented in **Figure 13**. Surprisingly, there is nearly no difference between this figure and the damping coefficient of the subsonic test case (Fig. 9), i.e. the maximum damping is overpredicted and, again, the minimum damping is matched very well. An explanation for this behaviour is given by the local work coefficient which is not shown here.

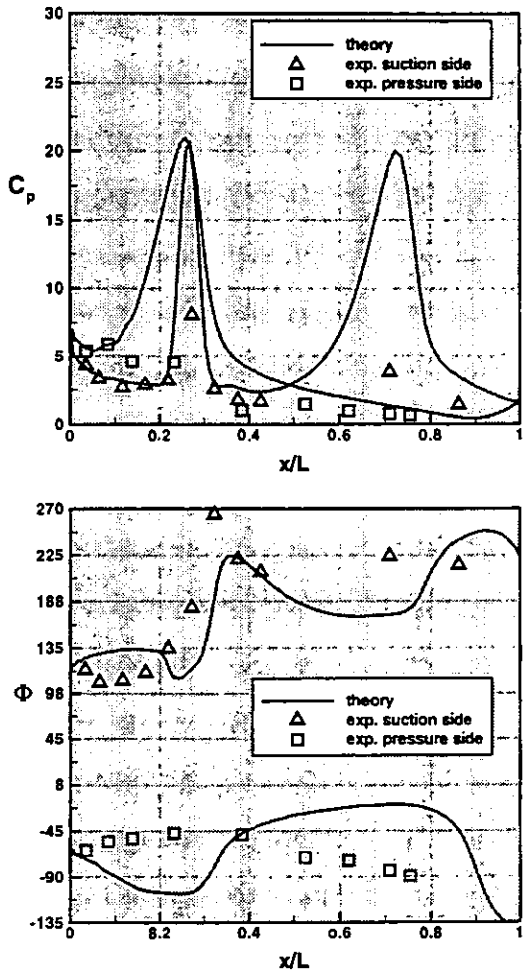

Figure 10: Unsteady pressure distribution, modulus and phase, Ma1 = 0.90, $\sigma = -90°$

For all three IBPA's this coefficient is positive (negative damping) where the blade passage shock impinges onto the suction side and negative (positive damping) where it impinges onto the pressure side. Thus, the overall aerodynamic work executed by the oscillating passage shock is very small and - if it is positive - always compensated by the positive damping contributions of the front shock and large regions of the pressure side.

CONCLUDING REMARKS

Numerical results of a method for computing the unsteady viscous flow around vibrating turbomachine blades have been compared with the experimental data of a transonic compressor cascade performing pitching oscillations around midchord. The experimental investigations were carried out in

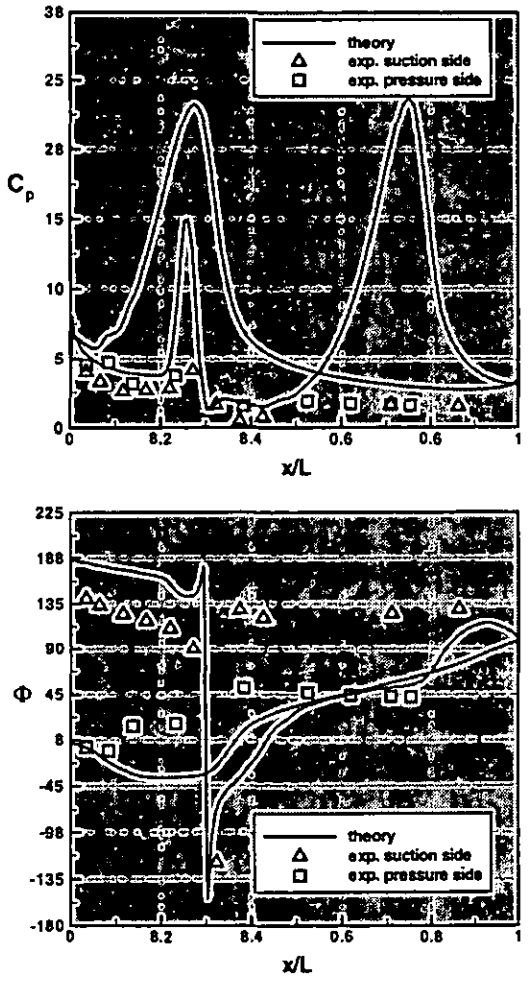

Figure 11: Unsteady pressure distribution, modulus and phase, Ma1 = 0.90, $\sigma = +90°$

an annular test facility where unsteady blade pressures were measured for subsonic and transonic flow. The corresponding theoretical results were computed with a Q3D Navier Stokes code, the special features of which are an upwind dicretization of the inviscid fluxes, the implementation of a one-equation turbulence model and the use of a multi-block deforming grid.

For the subsonic test case a reasonable agreement between computed and measured data is observed. Although the pressure amplitudes are overpredicted, the calculated pressure phases in general compare well with the measured ones. This is confirmed when comparing the numerical and experimental results for the damping coefficients where the agreement of the theoretical and measured value near the minimum damping is very good.

A more critical case is the prediction of unsteady pressures for transonic flow around the vibrating compressor blades. The computed steady pressure distrihution already differs significantly from the measured values indicating that possibly 3D effects play a role in this test case, i.e., that the assumption of a stream tube contraction on a constant radius may not be the best approximation of the real flow. The computed pressure amplitudes yield a pronounced response to the front shock and the blade passage shock and are much higher than the measured values. Additionally, the experimental results do not show the typical shock impulse at those locations where the blade channel shock impinges onto the pressure and suction surfaces. Despite these strong dicrepancies between computed and measured pressure amplitudes the agreement of predicted and experimentally determined pressure phases is satisfactory. Finally, it was found that the oscillations of the blade passage shock ohserved in this test case have nearly no influence on the aerodynamic damping of the blades.

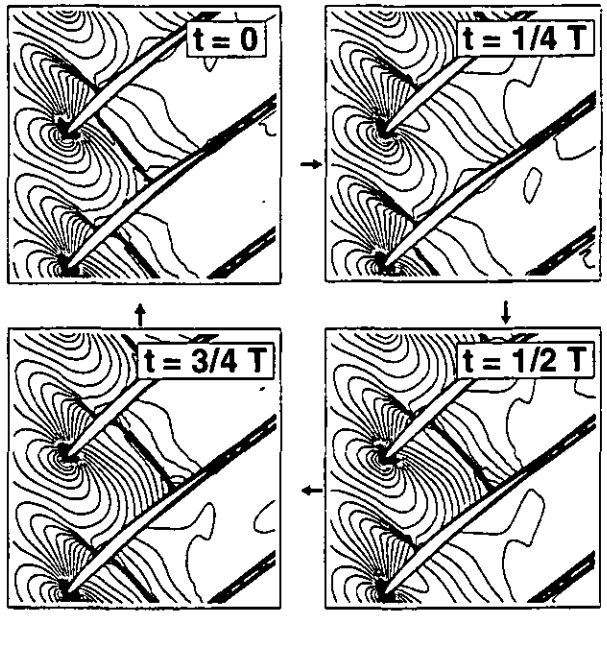

Figure 12: Iso-Machlines for unsteady flow at subsequent time-steps, Ma1 = 0.90, $\sigma = +90°$

ACKNOWLEDGEMENTS

This work is part of a joint research project with Daimler Chrysler Aerospace, MTU Munich. The cooperation with Dr. K. Heinig, Mr. G. Kahl and Dr. G. Fritsch and the permission to publish the results are gratefully acknowledged.

REFERENCES

Abhari, R. S. ; Giles, M. , 1995, *A Navier-Stokes Analysis of Airfoils in Oscillating Transonic Cascades for the Prediction of Aerodynamic Damping,* ASME Paper, 95-GT-182

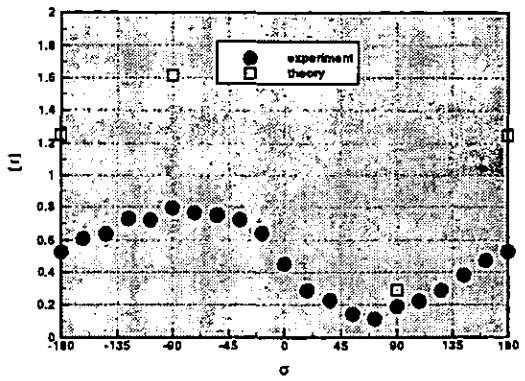

Figure 13: Aerodynamic damping coefficient versus interblade phase angle, transonic flow

Bölcs, A. ; Fransson, T.H. , 1986, *Aeroelasticity in Turbomachines - Comparison of Theoretical and Experimental Results,* Communications du Laboratoire de Thermique Appliquée et de Turbomachines, 13, EPFL, Lausanne

Carstens, V. ; Bölcs, A. ; Körbächer, H. , 1993, *Comparison of Experimental and Theoretical Results for Unsteady Transonic Cascade Flow at Design and Off-Design Conditions,* ASME Paper, 93-GT-100

Chuang, H.A. ; Verdon, J.M. , 1998, *A Nonlinear Numerical Simulator for Three Dimensional Flows through Vibrating Blade Rows,* ASME Paper, 98-GT-18

Clark, W.S. ; Hall, K.C. , 1995, *A Numerical Model of the Onset of Stall Flutter in Cascades,* ASME Paper, 95-GT-377

Eulitz, F. ; Engel, K. ; Pokorny, S. ; Faden, M. , 1996, *3D Navier-Stokes Solver for the Simulation of the Unsteady Turbomachinery Flow on a Massive Parallel Hardware Arcitecture,* Notes on Numerical Fluid Dynamics, Vieweg, Vol. 52

Eulitz, F. ; Engel, K. ; Gebing, H. , 1996, *Numerical Investigation of the Clocking Effects in a Multistage Turbine,* ASME Paper, 96-GT-26

Eulitz, F. ; Engel, K. , 1998, *Numerical Investigation of Wake Interaction in a Low Pressure Turbine,* ASME Paper, 98-GT-563

Gerolymos, G.A. , 1988, *Numerical Integration of the Blade-to-Blade Surface Euler Equations in Vibrating Cascades,* AIAA, Vol. 26, pp. 1483-1492

Gerolymos, G.A. ; Vallet, I. , 1994, *Validation of 3D Euler Methods for Vibrating Cascade Aerodynamics,* ASME Paper, 94-GT-294

Grüber, B. ; Carstens, V. , 1998, *Computation of the Unsteady Transonic Flow in Harmonically Oscillating Turbine Cascades Taking into Account Viscous Effects,* Journal of Turbomachinery, Vol. 120, No 1, pp. 104-111

Hall, K.C. ; Crawley, E.F. , 1989, *Calculation of Unsteady Flows in Turbomachinery Using the Linearized Euler Equations,* AIAA, Vol. 27, pp. 777-787

Hall, K.C. ; Lorence, C.B. , 1993, *Calculation of Three Dimensional Flows in Turbomachinery Using the Linearized Harmonic Euler Equations,* Journal of Turbomachinery, Vol. 115, No 4, pp. 800-809

He, L. , 1989, *An Euler Solution for Unsteady Flows Around Oscillating Blades,* ASME Paper 89-GT-279

He, L. ; Denton, J.D. , 1993, *Three Dimensional Time-Marching Inviscid and Viscous Solutions for Unsteady Flows Around Vibrating Blades,* ASME Paper 93-GT-92

He, L. , 1993, *New Two Grid Acceleration Method for Unsteady Navier-Stokes Calculations,* Journal of Propulsion and Power, Vol. 9, pp 272

Hennings, H. ; Belz, J. , 1998, *Experimental Investigation of the Aerodynamic Stability of an Annular Compressor Cascade Performing Tuned Pitching Oscillations in Transonic Flow,* To be published on ASME Turbo Expo 1999

Holmes, D.G. ; Mitchell, B.E. , Lorence, C.A., 1997, *Three Dimensional Linearized Navier-Stokes Calculations for Flutter and Forced Response,* Proceedings of the 8th International Symposium on Unsteady Arodynamics and Aeroelasticity of Turbomachines, Stockhom, Sweden, September 14-18

Kahl, G. ; Klose, A. , 1993, *Computation of the Linearized Transonic Flow in Oscillating Cascades,* ASME Paper 93-GT-269

Körbächer, H. , 1996, *Experimental Investigation of the Unsteady Flow in an Oscillating Annular Compressor Cascade,* Communication du Laboratoire de Thermique Appliquée et de Turbomachines, No 24, EPFL, Lausanne

Montgomery, M.D. ; Verdon, J.M. , 1997, *A 3D Linearized Unsteady Euler Analysis for Turbomachinery Blade Rows, Part 1 : Aerodynamic and Numerical Formulations, Part 2 : Unsteady Aerodynamic Response Predictions,* Proceedings of the 8th International Symposium on Unsteady Arodynamics and Aeroelasticity of Turbomachines, Stockhom, Sweden, September 14-18

Peitsch, D. ; Gallus, H.E. ; Weber, S. , 1994, *Computation of Unsteady Transonic 3D-Flow in Turbomachine Bladings,* Proceedings of the 7th International Symposium on Unsteady Arodynamics and Aeroelasticity of Turbomachines, Fukuoka, Japan, September 25-29

Weber, S. ; Benetschik, H. ; Peitsch, D. ; Gallus, H.E. , 1997, *A Numerical Approach to Unstalled and Stalled Flutter Phenomena in Turbomachinery Cascades,* ASME Paper, 97-GT-102